Lift forces on a circular cylinder in cross flow resulting from heat/mass transfer

Z. Trávníček[1], F. Maršík[2], T. Vít[1, 3], Z. Broučková[1] & M. Pavelka[1]
[1]*Institute of Thermomechanics AS CR, v.v.i., Prague, Czech Republic*
[2]*University of West Bohemia, Plzen, Czech Republic*
[3]*Technical University of Liberec, Czech Republic*

Abstract

The well-known Magnus effect is the phenomenon responsible for the curved streamlines around rotating cylinders or balls. In other words, the phenomenon causes the curved motion of spinning balls and missiles. A related application is the Flettner rotor ship, which was designed to use the Magnus effect for propulsion. More generally, the Kutta-Joukowski theorem determines lift as the product of upstream velocity, fluid density, and circulation. Flow visualization experiments of cylinders in a cross flow demonstrate this effect. For comparison purposes, a classical potential solution is presented with the same parameters (with the Reynolds number of 920). The present study assumes that similar effects can be created by means of a non-symmetrical heat/mass transfer from a section of the bluff body. A theoretical model was derived, based on equations of momentum, mass, and energy balance. The derivation utilized the terms of the entropy gradient, and the resulting velocity circulation around the body. A circular cylinder with a mass transfer surface was suggested. The mass transfer, namely the evaporation of water, is proposed through a selected 90° segment of the cylinder surface.
Keywords: cylinder in cross flow, Magnus effect, active flow control.

1 Introduction

The phenomena arising from the flow past a rotating body, such as the diversion of flying bullets or golf balls from their direct path, has been observed for several centuries.

WIT Transactions on Modelling and Simulation, Vol 55,
www.witpress.com, ISSN 1743-355X (on-line)
doi:10.2495/CMEM130131

The first experiments were performed in the middle of 19th Century by Heinrich Gustav Magnus, who confirmed the existence of additional forces in the flow past rotating bodies. The studied phenomenon was later named after him. The flow around a rotating cylinder was also investigated by Ludwig Prandtl in the first half of the 20th Century. For more details, see Zdravkovich [1].

This work focuses on the ability to generate circulation – and thus lift – by mass transfer, particularly via the evaporation of water from a segment of a cylinder. It is difficult to perform experiments in which the evaporation from the cylinder surface is well controlled. That is why this paper uses theoretical background and reference experiments of visualization of flow past rotating cylinders. To complement the context, the experiments are compared with a known mathematical model of potential flow.

2 Overview of the experiments

This paper presents the results of eight experiments conducted with two cylinders of different diameters, D. An overview of the experiments is presented in Table 1, where n is the rotation speed of the cylinder, f is the wake frequency measured by the stroboscope (no. 5, see part 4.1 below) or estimated (no. 1) from Eq. (15), v_∞ is the oncoming flow velocity, Re is the Reynolds number $Re = v_\infty D/\nu$, St is the Strouhal number $St = fD/v_\infty$, Γ is the circulation $\Gamma = n\,\pi^2 D^2$, F_v is the lift force form the Kutta-Joukowsky theorem (see Eq. (13) in the text below), and ν is the kinematic viscosity. Experiments 2 through 4 were performed with the cylinder rotating in a clockwise direction.

Table 1: Overview of the experiments.

no.	D mm	n Hz	f Hz	v_∞ m/s	Re	St	Γ m^2/s	F_v N
1	25.0	0	4.77	0.563	920	0.2118	0	0
2	25.0	5.0	-	0.563	920		-	0.0308 0.00057
3	25.0	12.5	-	0.563	920		-	0.0771 0.00144
4	25.0	20.0	-	0.563	920		-	0.1234 0.00230
5	3.0	0	31.8	0.563	110	0.1694	0	0

3 Potential flow model

The presented results show the solution of a two-dimensional flow of an ideally incompressible fluid without internal friction, i.e. zero viscosity is assumed. The importance of the model of potential flow in fluid mechanics comes from historical context (much older than practical using of computers) and from a visual interpretation of the influence of individual parameters on the results.

The potential flow velocity is defined by the potential function Φ or by the stream function Ψ. Both of these functions can be expressed as a function of a

single complex variable $F(z) = F(x + iy)$ in the case of planar flow. Function $F(z)$ is called the complex potential. The complex potential can be expressed as:

$$F(z) = \Phi(x, y) + i\Psi(x, y) \tag{1}$$

It is possible to derive the complex potential of a flow past a rotating cylinder as a superposition of free stream flow, dipole, and potential vortex.

Free stream flow: The complex potential function for free stream can be described as:

$$F(z) = v_\infty z. \tag{2}$$

Line source or sink: The complex potential function for a source or sink is:

$$F(z) = \frac{Q}{2\pi} \ln \frac{z}{r_0} \tag{3}$$

where Q is the flow rate (positive or outwards for a source, negative or inwards for a sink) and r_0 is the radius corresponding to the line with zero potential velocity.

Dipole is created by the superposition of a source and a sink of equal intensity placed symmetrically with respect to the origin. The complex potential of the dipole is:

$$F(z) = \frac{M}{2\pi} \frac{1}{z}, \tag{4}$$

where $M = 2Qx_0$ is the momentum of duplet and $2x_0$ is the distance between the source and sink.

Free vortex has a complex potential of:

$$F(z) = i\frac{\Gamma}{2\pi} \ln \frac{z}{r_0}, \tag{5}$$

where r_0 corresponds to the radius of the circle, the stream friction equals zero, and Γ is circulation defined as:

$$\Gamma = \oint v_t ds = 2\pi r v_t = (2\pi r)^2 n. \tag{6}$$

Quantity v_t is the velocity of the particle in a potential vortex. This velocity is tangential to the circle with radius r. The center of the circle is in the center of the vortex.

Rotating cylinder: Superposition of the free stream (2), dipole (4), and free vortex (5) leads to the formulation of a complex potential function for a rotating cylinder in which the center is situated at the center of a coordinates system. The complex potential is written as:

$$F(z) = v_\infty z + \frac{M}{2\pi} \frac{1}{z} + i\frac{\Gamma}{2\pi} \ln \frac{z}{r_0}. \tag{7}$$

This expression can be modified as:

$$F(z) = v_\infty z + v_\infty \frac{r_0^2}{z} + i\frac{\Gamma}{2\pi}\ln\frac{z}{r_0}. \tag{8}$$

Substituting $z = x + iy$ and separating the real and imaginary parts of Eq. (8), the potential function Φ and stream functionΨ are derived as:

$$\Phi = \left(1 + \frac{r_0^2}{x^2 + y^2}\right) v_\infty x - \frac{\Gamma}{2\pi} arctg\frac{y}{x}, \tag{9}$$

$$\Psi = \left(1 - \frac{r_0^2}{x^2 + y^2}\right) v_\infty y + \frac{\Gamma}{2\pi}\ln\frac{\sqrt{x^2 + y^2}}{r_0}. \tag{10}$$

Variable r_0 indicates (as in the case of a potential vortex) the radius of the circle that represents part of the line of zero stream function. This value indicates the radius of the cylinder.

Circulation affects the position of the leading and trailing point on the cylinder, i.e. the position of the points where the tangential velocity is zero. Tangential velocity is obtained as the negative value of the derivative of stream function by the radial coordinate r. The position of the leading and trailing points comes from the coordinates v_t $(r_0) = 0$. These points are symmetric along a vertical axis of the cylinder, and their vertical coordinate y_n is:

$$y_N = -\frac{\Gamma}{4\pi v_\infty}. \tag{11}$$

Equations (9) and (10) represent the functions for flow field past a stationary cylinder when the circulation is $\Gamma = 0$. Leading and trailing points are located on the x axis. A marginal case occurs when $\Gamma = 4\pi r_0 v_\infty$. In this case, leading and trailing points merge into one stagnation point on the surface. This stagnation point lies on the vertical axis. For higher values of circulation, the stagnation point separates from the cylinder surface and moves in the y direction. The distance of the point on the vertical axis from the origin of the coordinate system is:

$$y_N = \left|\frac{\Gamma}{4\pi v_\infty}\right| + \sqrt{\left(\frac{\Gamma}{4\pi v_\infty}\right)^2 - r_0^2}. \tag{12}$$

Lift force perpendicular to the free stream occurs in the case of a flow past a rotating cylinder. The magnitude of this force is represented by the well-known Kutta-Joukowsky theorem (e.g. [1]) as:

$$F_v = \rho v_\infty l\Gamma, \tag{13}$$

where l is the cylinder length.

Figure 1 shows the contours of the stream function Ψ (according to Eq. (10) for experiments 1 to 4 in Table 1). The cylinder was placed into the origin of the coordinate system. The oncoming flow of velocity v_∞ flows from left to right along the x axis. The same part of the flow field (the square of the dimensions: (-0.1, 0.1) x (-0.1, 0.1) m) is shown in all pictures.

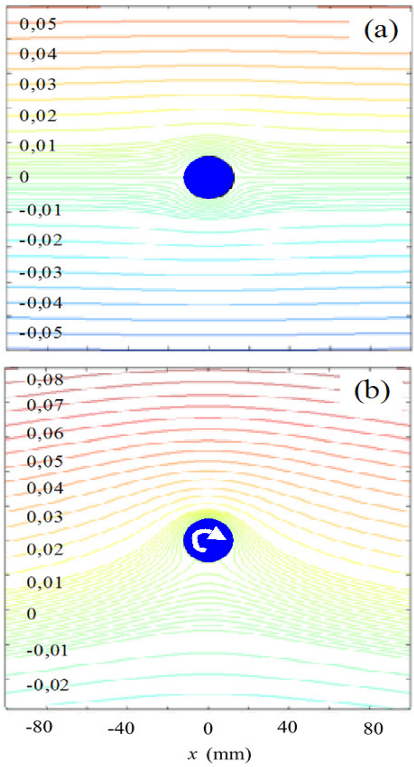

Figure 1: (a, b); for legend see next page.

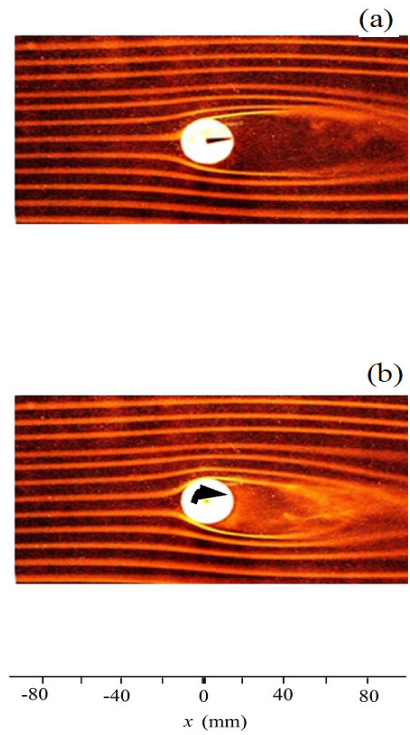

Figure 2: (a, b); for legend see next page.

The cylinder rotates in a clockwise direction. The finer step between contours, $\Delta\Psi = 0.001$, is set in proximity of the cylinder. Step $\Delta\Psi = 0.01$ is set for $\Psi > 0.01$ and $\Psi < -0.01$ respectively. The figures confirm previous conclusions. Stagnation points lie on the horizontal axis of a stationary cylinder – see Fig. 1(a). For a rotating cylinder, both points move downwards – see Fig. 1(b, c). The critical speed and the critical circulation, related to the only one stagnation point on the cylinder, are $n_{crit} = 2v_\infty/\pi D$ and $\Gamma_{crit} = 2\pi D v_\infty$ respectively. Namely, for the present case: $n_{crit} = 14.3\ s^{-1}$ and $\Gamma_{crit} = 0.0884\ m^2/s$.

Finally, in cases when the rotating speed is greater than the critical speed, the stagnation point separates from the cylinder surface and shifts downwards along the vertical axis – see Fig. 1(d).

4 Visualization of flow field

Visualization was performed in a small wind tunnel measuring 340 x 460 x 29 mm (length x height x depth). The cylinder for the visualization experiments had

a diameter of D = 25 mm and a length of l = 28 mm. Rotation was provided by a stepper motor with gearbox.

Water mist was used for visualization. The mist was created using a Mini Nebler ultrasonic fog generator and fed into the wind tunnel with a vertically perforated tube. The length of the tube corresponded to height of the workspace in the tunnel. The workspace of the tunnel was continuously illuminated. Flow patterns in the tunnel were photographed by a Canon PowerShot G7 camera, which was located at a distance of 0.7 meters from the front wall of the tunnel. Exposure time was 1 s, allowing the photographs to show the streaklines of the flow.

Because flow velocity was relatively small (v=0.563 m/s, see the part 4.1 below), water drops descending from the mist due to gravity were observed to have a slight slope in their trajectory. The slope was approximately 3° in all of the experiments. The pictures presented in this paper are therefore rotated anti-clockwise to eliminate this angle.

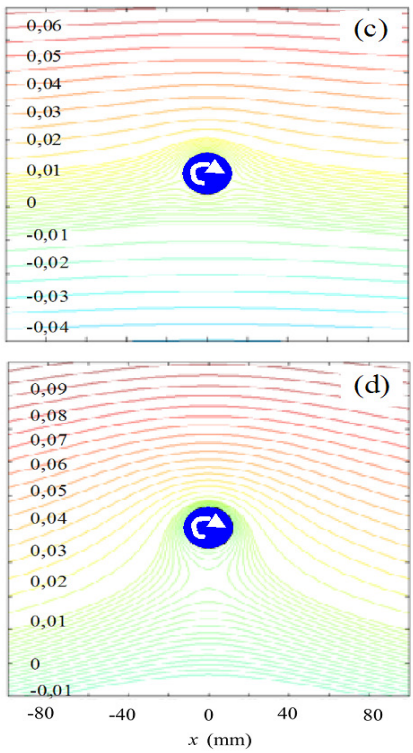

Figure 3: Potential theory contours of the stream function Ψ, (a) n=0, (b) n=5 s^{-1}, (c) n=12.5 s^{-1}, (d) n=20 s^{-1}.

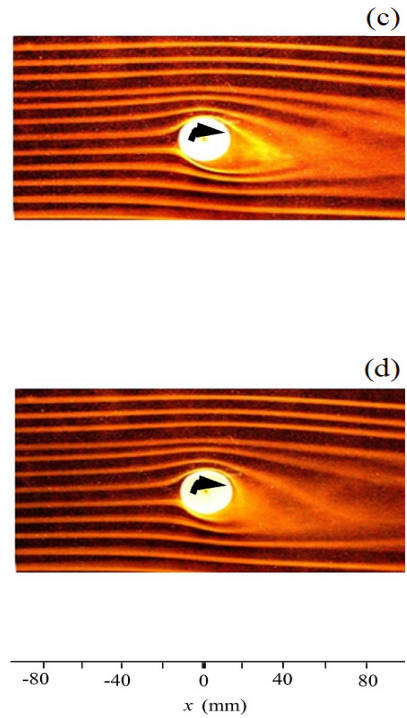

Figure 4: Flow visualization for the same rotation speed n as in Fig. 1. Exp. parameters – see no. 1–4 in Table 1.

Figure 2 shows a visualization of experiments 1 to 4 according to Table 1. The cylinder was rotated in a clockwise direction. Experiments with a stationary cylinder are shown in Fig. 2(a). Vortex shedding is roughly symmetrical along the horizontal axis of the cylinder. Figure 2(b–d) shows flow patterns in cases using a rotating cylinder. The deflection of the flow due to the rotation of the cylinder, as well as the shift of the separation point with an increase in the speed of rotation, is evident.

Comparison of the results from visualization experiments with the potential theory (Fig. 1) shows that the potential flow due to its simplistic assumptions (incompressible fluid without internal friction) gives only an approximate idea of the flow field past stationary and rotating cylinders. It can be seen that the viscosity and related phenomena, such as the existence of laminar or turbulent flow, plays an important role in flow past a body.

Note, that this work is primarily focused on the study of time-averaged flow fields. The vortex shedding frequency in the wake of the rotating cylinders was not dealt with in this study. Therefore, the corresponding parameters are not provided in Table 1.

4.1 Evaluation of flow velocity of oncoming flow from shedding frequency

Velocity of the oncoming flow was evaluated by experiment no. 5 (Table 1). A stroboscope (Cole Palmer 87002) was used to illuminate the working space of the wind tunnel during the experiment. The strobe frequency was synchronized with the shedding frequency of vortices in the cylinder wake. Figure 3 shows the results of visualization. It must be mentioned that this picture shows a multiexposition of 31 images captured with at stroboscope frequency of 31.8 Hz. Therefore, Fig. 3 confirms the excellent periodicity of the phenomenon.

The Williamson and Brown [2] formula:

$$St = C_1 - C_2 / \sqrt{Re}\,, \tag{14}$$

can be used to evaluate the velocity of oncoming flow from the observed shedding frequency, where C_1 and C_2 are constants with values C_1 = 0,2665 and C_2 = 1,0175 for Re = (49÷180), and C_1 = 0,2234, C_2 = 0,3490 for Re = (230÷1200).

Only slightly different values of C_1 and C_2 in Eq. (14) can be found in the work of other authors, e.g. Fey *et al.* [3] or Wang *et al.* [4].

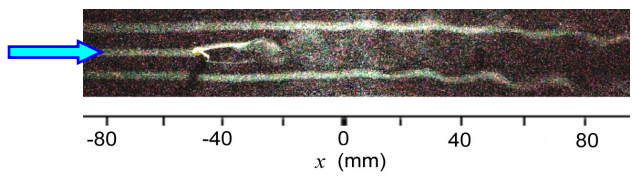

Figure 5: Flow visualization of the von Kármán vortex street at Re = 110, multiexposition of 31 images, at f = 31.8 Hz (experiment no. 5, Table 1).

Substituting *St* and *Re* to Eq. (14) the formula for the oncoming velocity of v_∞ is:

$$v_\infty = \frac{1}{4}\left(-b + \sqrt{b^2 - 4c}\right)^2, \tag{15}$$

where $b = \frac{C_2}{C_1}\sqrt{\frac{\nu}{d}}$ and $c = -\frac{fd}{C_1}$.

The shedding frequency was measurement by the stroboscope and the result was f = 31.8 Hz. Then the oncoming velocity and the Reynolds number were evaluated as v_∞ = 0.563 m/s and *Re* = 110, respectively.

5 Relation between force interaction and heat transfer

Equations of conservation of mass, momentum, and total energy in classical fluid mechanics are usually formulated as the balance laws of the corresponding quantities. The second law of thermodynamics is understood as the balance of entropy. A completely different physical interpretation of the balance of momentum follows from the modified Lagrange principle of classical mechanics with application to fluids. The relevant correlation between the classical mechanics of material points and classical continuum mechanics can be established when the existence of a trajectory and a friction force are added. The relation between friction force and the rotational part of a velocity field derived from the Lagrange principle allows the balance of momentum for a stationary flow to be formulated as follows

$$\mathbf{v} \times \text{rot}\,\mathbf{v} = \text{grad}\,h_c - T\text{grad}\,s - \text{grad}\,\phi \tag{16}$$

where the total enthalpy h_c is defined as the sum of kinetic energy $\mathbf{v}^2/2$, internal energy *u*, pressure energy p/ρ, and the potential energy of the external volume forces ϕ

$$h_c = \frac{\mathbf{v}^2}{2} + u + \frac{p}{\rho} + \phi \tag{17}$$

The total enthalpy for the stationary case is constant. Under the same conditions, the balance of momentum in classical fluid mechanics is formulated as:

$$\mathbf{v} \times \text{rot}\,\mathbf{v} = \text{grad}\,h_c - T\text{grad}\,s - \frac{1}{\rho}\text{div}\,\mathbf{t}_{\text{dis}} \tag{18}$$

which is the so-called Crocco theorem. The dissipative part of the Cauchy stress tensor for Navier-Stokes fluid is:

$$\mathbf{t}_{\text{dis}} = \mu(\rho, T)\left(\text{grad}\,\mathbf{v} + (\text{grad}\,\mathbf{v})^{\text{T}} - \frac{2}{3}(\text{div}\,\mathbf{v})\mathbf{I}\right) \tag{19}$$

where the viscosity $\mu(\rho,T)$ is crucial fluid quality, which generates the force interaction between the fluid and a solid wall. Solely due to viscosity, the velocity gradient on the wall of the rotational cylinder can only be generated in the boundary layer, see Fig. 4,

$$t_{r\varphi} = \mu\left(\frac{\partial \mathrm{v}_\varphi}{\partial r} - \frac{\mathrm{v}_\varphi}{r}\right)\Bigg|_{r\in(R,R+\delta)} \tag{20}$$

and, consequently, the rotational part of the velocity field is:

$$\mathrm{rot}\,\mathbf{v} = \left(\frac{\partial \mathrm{v}_z}{r\partial\varphi} - \frac{\partial \mathrm{v}_\varphi}{\partial z}, \frac{\partial \mathrm{v}_r}{\partial z} - \frac{\partial \mathrm{v}_z}{\partial r}, \frac{\partial\left(r\mathrm{v}_\varphi\right)}{r\partial r} - \frac{\partial \mathrm{v}_r}{r\partial\varphi}\right)\Bigg|_{r\in(R,R+\delta)} = \left(0,0,\frac{\partial \mathrm{v}_\varphi}{\partial r}\Big|_{r\in(R,R+\delta)}\right) \tag{21}$$

According to Eq. (18), the volume force on the fluid in the boundary layer has a radial direction only:

$$\left(\mathbf{v}\times\mathrm{rot}\,\mathbf{v}\right)_r = \left(\mathrm{v}_\varphi\frac{\partial \mathrm{v}_\varphi}{\partial r}\right)_{r\in(R,R+\delta)} \sim -\frac{\mu}{\rho}\frac{\partial^2 \mathrm{v}_\varphi}{r\partial\varphi\partial r}\Bigg|_{r\in(R,R+\delta)} \tag{22}$$

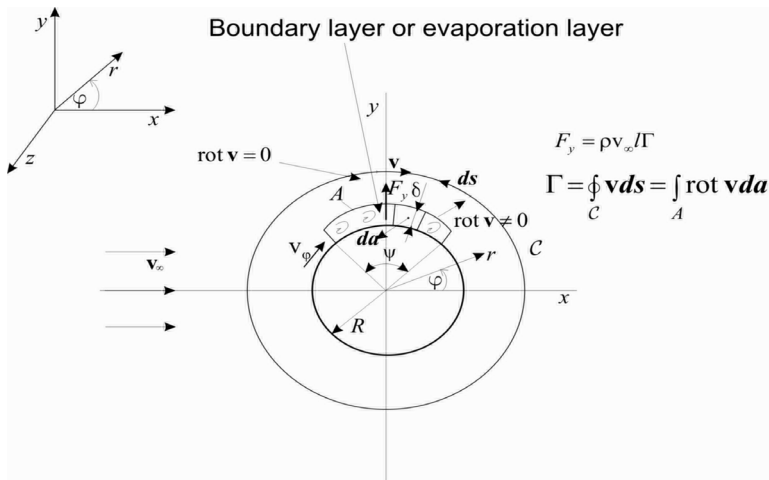

Figure 6: The circulation Γ generated by the velocity field with the rot $\boldsymbol{v} \neq 0$ induces the lift F_y.

The circulation Γ, which is generated inside the boundary layer by the $\mathrm{rot}\,\mathbf{v} \neq 0$ part, can be alternatively generated by a change in entropy as follows from Eqs. (16) and (18):

$$\left(\mathbf{v}\times\mathrm{rot}\,\mathbf{v}\right)_r = \left(\mathrm{v}_\varphi\frac{\partial \mathrm{v}_\varphi}{\partial r}\right)_{r\in(R,R+\delta)} \sim T\mathrm{grad}_r s \sim \frac{h_{evap}}{\delta} \tag{23}$$

where h_{evap} [J/kg] is the specific evaporation heat, which is negative.

With respect to the estimation of $(\mathrm{rot}\,\mathbf{v})_z$ in Eq. (21), together with Eq. (23), the circulation can be approximately evaluated as follows:

$$\Gamma = \oint_{\mathcal{C}} \mathbf{v}\,\mathrm{d}s = \int_A \mathrm{rot}\,\mathbf{v}\,\mathrm{d}\mathbf{a} \sim \int_A \frac{\partial \mathrm{v}_\varphi}{\partial r}\,\mathrm{d}\mathbf{a} \sim \frac{h_{evap} A}{\mathrm{v}_\varphi \delta} \tag{24}$$

The cross-section of the evaporation layer is $A = \psi R\delta$. For $\psi = \pi/2$, the tangential velocity is $\mathrm{v}_\varphi \in (1.41, 2)\,\mathrm{v}_\infty$. It can be estimated using a coefficient of $a \in (1.41, 2)$, so that $\mathrm{v}_\varphi = a\mathrm{v}_\infty$.

Circulation around the cylinder can be generated by cylinder rotation as well. Applying Eq. (24) gives:

$$\Gamma = (2\pi R)^2 n = \frac{\psi R h_{evap}}{a\mathrm{v}_\infty} \tag{25}$$

and the corresponding number of rotations can be estimated as:

$$n = \frac{\psi h_{evap}}{(2\pi)^2 a R \mathrm{v}_\infty} \quad \left[\mathrm{s}^{-1}\right] \tag{26}$$

The specific evaporation heat of water at 18°C is $h_{\mathrm{lv}} = 2458$ kJ/kg. The evaporation heat needed to generate circulation is $h_{evap} = \Delta c_{\mathrm{v}} h_{\mathrm{lv}}$ and is induced by a change in air humidity Δc_{v}, where $c_{\mathrm{v}} = \rho_{\mathrm{v}} / (\rho_{\mathrm{a}} + \rho_{\mathrm{v}})$ is the mass concentration of the water vapor in the air.

6 Conclusion

This work deals with the flow fields around stationary and rotating cylinders at *Re* = 920. Visualization was performed using a water mist in a small wind tunnel. The visualization of the von Kármán vortex street in the wake of cylinder at *Re* = 110 is also presented. A measured shedding frequency was used to evaluate velocity of oncoming flow in the wind tunnel.

A mathematical model of the flow field based on analysis of potential flow is also presented in this paper. It has been shown that viscosity has a significant influence on the character of the flow, and the potential flow model can not fully describe real flows.

Finally, a theoretical model was derived, focusing on generation by means of non-symmetrical mass transfer (water evaporation) from a part of the bluff body.

Acknowledgements

We are sincerely grateful for the support of the GAAS CR (No. IAA200760801), CENTEM project, reg. no. CZ.1.05/2.1.00/03.0088, which is partially supported by the ERDF within the OP RDI Programme of the Ministry of Education, Youth and Sports, and GACR (No. P101/11/J019). We would also like to thank Petr Jerie for preparing the wind tunnel and for putting it into operation.

References

[1] Zdravkovich, M.M., Flow around Circular Cylinders, Volume 2, Oxford University Press: New-York, 2003.

[2] Williamson, C.H.K and Brown, G.L., A series in $(1/\sqrt{\mathrm{Re}})$ to represent the Strouhal–Reynolds number relationship of the cylinder wake. Journal of Fluids and Structures, 12(fl980184), pp. 1073–1085, 1998.

[3] Fey, M., Kőnig, M. and Eckelmann, H., A new Strouhal–Reynolds number relationship for the circular cylinder in the range 47<Re<2x105. Physics of Fluids, 10(7), pp. 1547–1549, 1998.

[4] Wang, A.-B., Trávníček, Z. and Chia, K-C., On the relationship of effective Reynolds number and Strouhal number for the laminar vortex shedding of a heated circular cylinder. *Physics of Fluids*, **12(6)**, pp. 1401-1410, 2000.